

SIMULATIONS OF AEROSOLS AND PHOTOCHEMICAL SPECIES WITH THE CMAQ PLUME-IN-GRID MODELING SYSTEM

J. M. Godowitch
Atmospheric Sciences Modeling Division, Air Resources Laboratory
National Oceanic and Atmospheric Administration
Research Triangle Park, North Carolina
email: godowitch.james@epa.gov

1. INTRODUCTION

A plume-in-grid (PinG) treatment has been an integral component of the Community Multiscale Air Quality (CMAQ) modeling system. The PinG approach was designed to provide a realistic treatment of the dynamic and chemical processes governing pollutant concentrations in the plumes emitted from the selected major point source stacks on the subgrid scale. For large regional or continental modeling domains, in particular, grid cell sizes are generally specified to be tens of kilometers on a side. However, due to their small spatial extent in the horizontal dimension, point source plumes are a subgrid scale feature on a typical Eulerian grid modeling framework. Consequently, artificial dilution is considerable when point source emissions are instantly mixed into a large grid cell volumes, which impacts primary pollutant concentrations and the chemical processes governing secondary species. In contrast, the PinG technique spatially resolves the large concentration gradients within plumes by simulating the gradual growth downwind using a Lagrangian framework. Since the plumes are modeled at the proper spatial scale, chemical processes in the plume evolve in a more realistic manner.

This paper contains an overview of the key components of the current CMAQ plume-in-grid modeling system. A description of the procedures to perform model simulations with the PinG treatment will also be given. In previous public releases of the CMAQ modeling system, the PinG module was capable of treating photochemical processes. A notable update in the current release version of the CMAQ/PinG is the inclusion of a treatment for aerosol formation processes. Model results of selected photochemical and aerosol species from a test application are also presented to illustrate the impact on the gridded concentration field.

2. MODEL OVERVIEW

The key modeling components of the CMAQ PinG approach are the plume dynamics model (PDM) processor program and the PinG module, which is a Lagrangian reactive plume model. A technical description of the relevant plume processes treated in these PinG algorithms and

their mathematical formulations have been documented in Gillani and Godowitch (1999). The PDM processor generates a data file containing plume position and plume dimension information for the PinG module, which is fully integrated inside the CMAQ Chemical Transport Model (CTM). To be consistent, the PinG module applies the same chemical mechanisms (i.e. CB-IV, SAPRC-99) as the CTM. The current version of the CMAQ/PinG applies the GEAR chemical solver (Gipson and Young, 1999), which provides an accurate solution for the high NO_x concentration regime found in many point source plumes. The current CMAQ aerosol module (Binkowski, 1999) applied in the CTM has been incorporated into the PinG module to provide a treatment of aerosol processes in the subgrid plumes. The Binkowski aerosol algorithm represents the size distribution by the superposition of 3 lognormal subdistributions (i.e. modes). Relevant processes are considered that impact PM_{2.5}, PM₁₀, and secondary aerosol species including sulfate (SO₄⁻²), nitrate, ammonium, water, and organics from precursors of anthropogenic and biogenic sources.

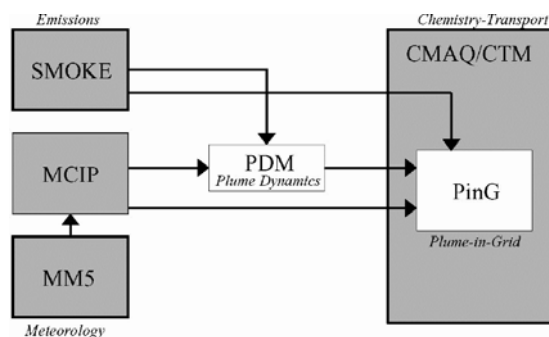


Figure 1. Flow diagram of the key plume-in-grid modeling components (PDM processor and PinG module) in the CMAQ modeling system.

The flow diagram in Figure 1 illustrates the two plume-in-grid modeling components. The PDM processor program shown in Figure 1 requires a stack parameter file created by a SMOKE emissions processor and the meteorological data files generated by the Meteorology Chemistry Interface Processor (MCIP). Therefore, when the PinG treatment will be applied, the first step begins during processing with the SMOKE emissions modeling system. Various criteria for emissions and/or stack parameter available to the user must be applied when executing the SMOKE

ELEVPOINT processor. Based upon input criteria, certain major point sources are designated as PinG sources. Emission rate criteria are generally specified in order to select the largest point sources in an inventory. For example, 47 point sources were identified from the 1999 inventory as PinG point sources since their emission rates for NO_x emission rate were greater than 75 tons/d or their SO₂ emission rates were greater than 150 tons/d. An output stack file (i.e. stack_groups file) contains the stack parameters of the major point sources to be treated later in the CTM/PinG simulation. This stack_groups files is also applied during the SMOKE merge step in order to generate the companion PinG emissions file.

The PDM processor simulations are performed in advance of the CTM/PinG modeling runs since PDM generates a data file (i.e., PDM_PING_1) needed by the PinG module. In particular, PDM is executed for a 24-hour period and it contains methods to compute plume rise, horizontal and vertical dimensions of each plume section, plume grid positions, and an important plume flag (IPLMFLG) variable. In particular, the IPLMFLG signals the PinG module when to initialize a new plume section and when to end the simulation of a particular plume section, which triggers the feedback of plume material to the CTM grid. The PDM code also has the capability to continue active plumes into the next day. Consequently, for processing cases after the first day, an environment variable in the run script (IOLDFIL) is revised from 0 to 1, and the PDM data file from the previous day (i.e., PDM_PING_0) is read in order to properly initialize the PinG module with active plumes at the start of the current simulation day. The PDM processor is executed for each day of a simulation period. Finally, the number of PinG sources currently allowed must be less than 100.

As with other process modules, the PinG algorithm is included in the CTM by the user when building the model executable code. The PinG emissions file (i.e., MEPSE_1), MCIP data files, 3-D emissions file (i.e., EMIS_1), and the PDM output file (i.e., PDM_PING_1) are used during execution of the PinG module. The plume concentration file generated by the PinG module contains the species concentrations in all plume cells of each active, subgrid scale plume section. A default set of 8 plume cells resolves the horizontal cross-section of a plume section. A separate PinG 2-D dry deposition output file is also generated containing the species deposition in the grid cells where the active plume sections are located. After completion of a CTM/PinG simulation run, a postprocessor program is available to merge the subgrid scale plume concentration file (CTM_PING_1) and the CTM gridded concentration field. The current PinG module is not applicable for model grid resolutions below about 12 km.

3. MODEL TEST SIMULATIONS

The model domain defined for CTM/PinG test simulations consisted of 21 x 21 horizontal grid cells with a 36 km grid cell size and 21 vertical layers. The PDM processor and CTM/PinG model runs were performed for a series of days in July 1995, which coincides with an intensive field study period conducted within the region. In the PinG module, photochemical processes were treated with the CB-IV chemical mechanism using the Gear solver and aerosol formation was modeled with the same aerosol algorithm (AE3) also applied in the CTM. For these simulations, the PinG module was applied with a set of 10 attached cells (5 on each side of the plume centerline) to resolve the horizontal plume cross-section.

Although the results presented herein are from a particular case (i.e., July 7, 1995), the findings are indicative of those found on other days from the modeling period. Five major point sources were selected for the plume-in-grid treatment. The point source emissions treated in PinG were from the Shawnee (SH), Paradise (PA), Cumberland (CU), Johnsonville (JV), and Gallatin (GA) fossil-fuel power plants. Total emissions from continuous monitoring measurements (CEM) for July 7, 1995 in Table 1 reveal a large range in the NO_x and SO₂ emissions among these point sources. The SO₂/NO_x ratio also differs greatly, which should provide an interesting variation among the photochemical and aerosol species concentrations for this set of sources.

TABLE 1.

Source	NO _x /NO _x (GA)	SO ₂ / NO _x
GA	1.0	7.3
JV	2.0	6.0
SH	2.9	2.3
CU	14.8	0.13
PA	14.9	1.7

Trajectories and growth of plume sections released at 1500 UTC on July 7, 1995 from these point sources are shown in the modeling domain in Figure 2. Due to the steady northwesterly flow on this day, the point source plumes were transported in parallel to each other. Other hourly plume releases also followed similar paths, which will assist in the interpretation of concentration field differences to be displayed later. The downwind movement of each plume section in Figure 2 is in 15 minute increments for the active, subgrid scale phase. During the PinG simulation, boundary concentrations are provided by the CTM grid cell concentrations where each plume section is situated. At this grid resolution, it is evident that these plume sections were subgrid scale for several grid cells downwind of their source locations. Once a plume section's width reaches the grid cell size, the PinG simulation of it ends and a feedback to the grid occurs.

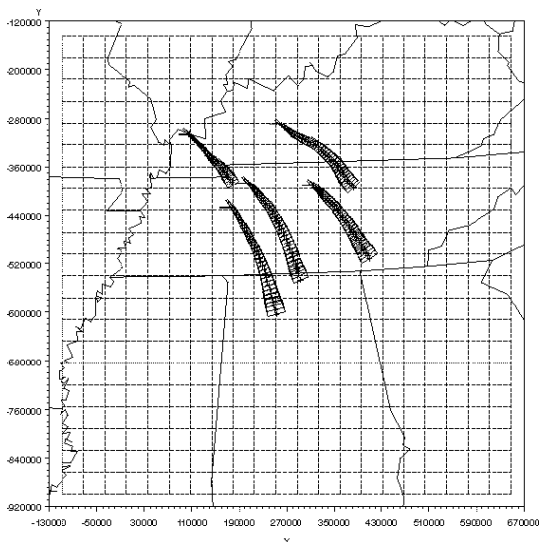


Figure 2. Trajectory and growth of the plume sections released at 1500 UTC on 7 July 1995 on the modeling domain with a 36 km grid cell size.

Figures 3 and 4 display selected species concentrations in the plume sections from a high NO_x , low SO_2 source (CU), and a lower NO_x , high SO_2 source (JV), respectively, at 5 hours after initialization (release time was 1500 UTC). Note the plume widths at this time are around 20 km, which is still much less than the grid cell size. The chemistry in the high NO_x plume in Figure 3 strongly favored HNO_3 formation and O_3 in the plume core continues to recover from a huge initial deficit due to the high NO emissions. Fine aerosol sulfate (SO_4^{2-}) is only slightly above background and the hydroxyl radical (OH) values are lower in the middle of the plume compared to the plume edges. In contrast, higher sulfate values were found in the JV plume, which also exhibited higher SO_2 concentrations. Due to lower NO_x emissions, considerably less HNO_3 was formed in the JV plume. In addition, excess O_3 above background existed in the JV plume core, while more time was needed for an O_3 excess to develop in the CU plume. Modeled gaseous species were found to be comparable to airborne plume measurements for this case (Godowitch, 2001).

Results illustrating aerosol sulfate in the center of plume sections for the releases at 1500 UTC from these sources are shown in Figure 5. Interestingly, the two highest NO_x sources with differing SO_2 emissions yielded the lowest sulfate concentrations above background values supplied by CTM. It is believed the more rapid reaction of NO_2 with OH caused less OH to be available for the slower SO_2 reaction with OH . As a result, sulfate formation is depressed in the higher NO_x plumes. Indeed, higher SO_4 levels were found in the point source plumes exhibiting higher SO_2 emissions coupled with lower NO_x emissions. These results are in agreement with emerging observational aerosol data from plumes (Brock et al, 2002).

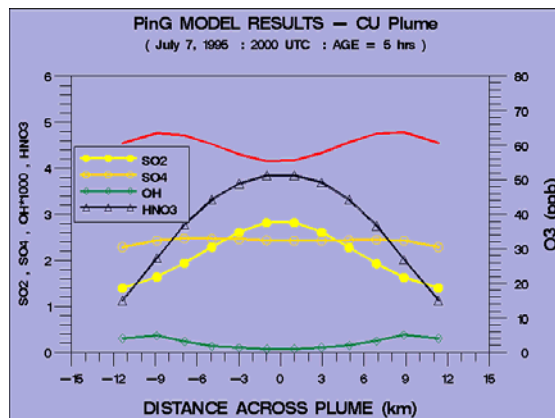


Figure 3. Selected species concentrations in the plume section from a high NO_x / low SO_2 emission source (CU) at 5 hours after release. Ozone (O_3) is the solid red line. Units: SO_4 ($\mu\text{g}/\text{m}^3$), OH (ppt), SO_2 and HNO_3 (ppb).

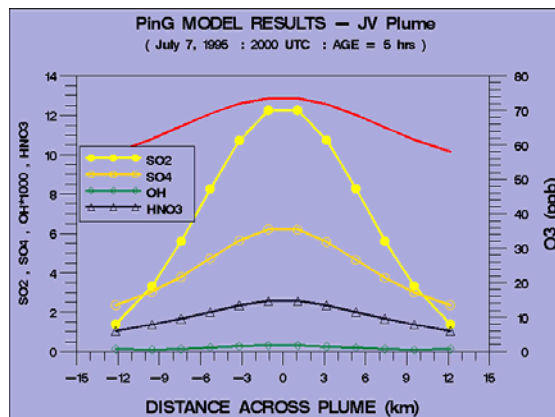


Figure 4. Selected species concentration in the plume section from a high SO_2 emission source (JV) at 5 hours after release, otherwise, same as Fig. 3.

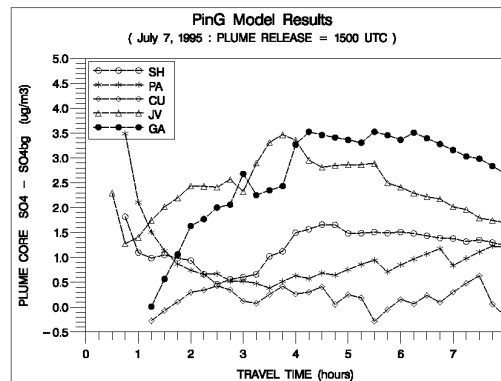


Figure 5. Aerosol sulfate concentrations relative to background in the center of plume sections with travel time from releases at 1500 UTC on July 7.

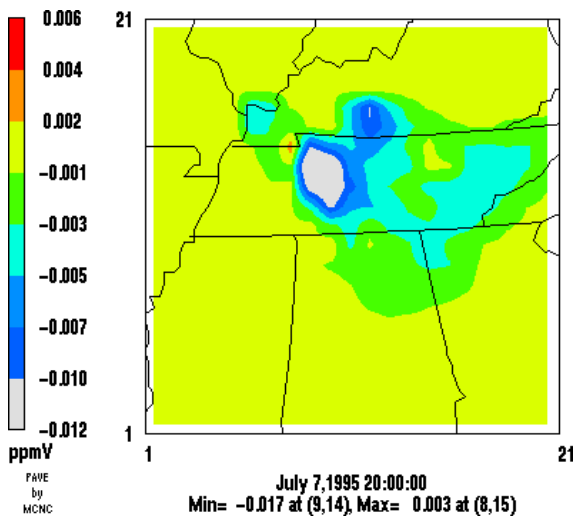


Figure 6. Ozone difference field determined by subtracting the CTM/NoPinG from the CTM/PinG concentration results.

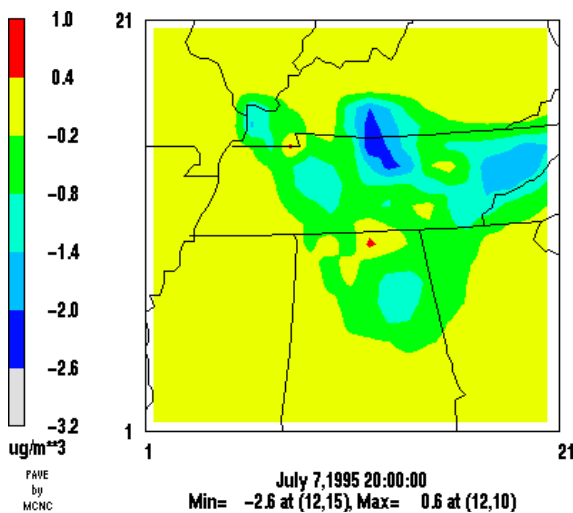


Figure 7. Aerosol sulfate (SO₄) difference field determined by subtracting the CTM/NoPinG from the CTM/PinG concentrations at the same afternoon hour in Figure 6.

Two sets of model runs were performed; one series applied the PinG treatment for the above group of point sources and another series without the PinG module. The results for ozone from the CTM/NoPinG simulation (not shown) revealed an O₃ maximum within and immediately downwind of the source locations due to the notable dilution of the NO_x emissions, which accelerated photochemical formation of ozone. The O₃ differences between the two runs shown in Figure 6 reveal lower O₃ concentrations in the CTM/PinG results, particularly in the grid cells in the vicinity of the two largest NO_x sources located in Kentucky and central Tennessee. Further downwind, ozone differences are smaller. The model results for aerosol sulfate in Figure 7 are somewhat similar, but strongly dependent on the

SO₂ emission strength of the source. Nevertheless, slightly lower SO₄ concentrations are found near the point source locations as well as further downwind in the areas where plume section handovers to the grid model had occurred.

4. SUMMARY AND ONGOING WORK

Photochemical and aerosol test simulation results with the updated CTM/PinG model are encouraging. The PinG treatment has already demonstrated a capability of capturing the observed photochemical behavior of O₃ and other gas species. The aerosol sulfate formation in the SO₂-rich model plumes also appears to be similar to observed plume findings. However, more analysis is warranted and comparisons with observed plume aerosol data are planned. Grid-scale concentration differences are apparent from model runs with/without the PinG approach. CTM/PinG simulations on a continental domain with speciated PM point source emissions are underway and results are anticipated at a future meeting.

DISCLAIMER

The research presented here was performed under the Memorandum of Understanding between the U.S. Environmental Protection Agency (EPA) and the U.S. Department of Commerce's National Oceanic and Atmospheric Administration (NOAA) and under agreement number DW13921548. Although it has been reviewed by EPA and NOAA and approved for publication, it does not necessarily reflect their policies or views.

REFERENCES

Binkowski, F.S., 1999: Aerosols in Models-3 CMAQ. Chap. 10 of Science Algorithm of the EPA Models-3 Community Multiscale Air Quality Modeling System. EPA/600.R-99.030, Research Triangle Park, NC.

Brock, C. A. et al., 2002: Particle growth in the plumes of coal-fired power plants. *J. Geo. Res.*, 107, D12,10.1029/2001D001062.

Gillani, N.V. and J.M. Godowitch, 1999: Plume-in-grid treatment of major point source emissions. Chap. 9, Science Algorithms of the EPA Models-3 CMAQ Modeling System. EPA/600/R-99/030, Research Triangle Park, NC.

Godowitch, J.M., 2001: Results of photochemical simulations of subgrid scale point source emissions with the Models-3 CMAQ modeling system. Preprints, AMS Millennium Symposium on Atmos. Chem., 14-19 Jan. 2001, Albuquerque, NM, p. 43-49.